J Opt (February 2024) 53(1):10–17
https://doi.org/10.1007/s12596-023-01125-w

RESEARCH ARTICLE

Preparation and characterization of acid green 50 dye–PVA composite films and their optical power limiting characteristics

S. Hemalatha[1] · T. Geethakrishnan[1]

Received: 26 May 2022 / Accepted: 1 February 2023 / Published online: 4 March 2023

Abstract In this paper, we present the preparation and characterization of acid green 50 dye–PVA composite films and their optical power limiting characteristics. UV–Visible spectroscopy (UV–Vis), x-ray diffraction (XRD), scanning electron microscope (SEM), and Fourier-transform infrared spectroscopy (FT-IR) were carried out to study the AG 50–PVA composites. The optical absorption spectra show a good linear absorption at 650 nm wavelength due to the presence of π–conjugated electrons in the AG 50 dye molecules. The XRD and FTIR studies were used to explain the interaction of AG 50 dye molecules with PVA, and SEM validated the morphological aspects. A continuous wave diode laser (CW) works at 635 nm wavelength with 5 mW output power was used to investigate the nonlinear absorption (NLA) of AG 50–PVA composite films via open aperture Z-scan technique. AG 50–PVA composite films have a high optical limiting efficiency due to strong reverse saturable absorption at this wavelength, making them potential candidates for eye and sensor protection devices. These low-cost, versatile, and environmentally friendly AG 50–PVA films hold promise to produce efficient optical devices for photonic applications.

Keywords Dye–PVA composites · Z-scan · Optical power limiting

✉ T. Geethakrishnan
tgeethakrishnan@hotmail.com

[1] Department of Physics, University College of Engineering Villupuram (A Constituent College of Anna University), Villupuram, Tamilnadu 605103, India

Introduction

Nonlinear optical properties (NLO) of different materials are being explored in depth and are of major value due to their potential applications in a variety of aspects of science and informatics. Organic NLO materials are being extended to polymers, which have piqued the interest of NLO researchers due to their high delocalized π-electron systems, fast response and large optical nonlinearities. Such functional NLO materials are of special interest in optical communications, optical storage, optical computing, harmonic generation, optical switching, and optical power limiting [1–6]. Organic dyes are encapsulated in polymer which create a new type of material with strong nonlinear and linear optical characteristics. Polymer-based systems have a high optical damage threshold, are transparent, and have a cheap processing cost. Polyvinyl alcohol (PVA) is a viable contender for opto-electronic applications because of its facile film forming ability, simplicity of insertion of dopants, sensing property, biocompatibility, and capacity to encapsulate unstable nanoparticles [7]. Several studies on the impregnation of organic dyes with polymers to produce films with anticipated optical characteristics have been reported in the literature. PVA–Au [8], Eosin Y–PVA and Eriochrome black T–PVA [9], PVA–TiO_2–CDs [10], Thiazole yellow G–PVA [11], red BS dye–PVA [12] and Zn O–PVA [13] are only a few of the synthetic dyes that have been recently studied. Similarly, poly(methyl methacrylate) (PMMA), polyethylene glycol (PEG) and other host materials have been used in the majority of dye-doped composites studies [14, 15]. Low mechanical strength, thermal instability and solvent volatility are all described as constraints for the synthetic dyes.

Acid green 50 (AG 50), a triarylmethane (TAM) dye, was chosen as the experimental dye for this study. TAM dyes are important class of synthetic organic dyes, which have

a highly delocalized π-conjugated electron system in both central carbon atom and the substituents on the aryl rings. These dyes have massive applications in optical switching, organic light emitting diodes, photovoltaic devices, photocatalysis, chemical biology, pharmaceutical chemistry, light harvesting systems and in nano technology [16, 17]. This AG 50 dye is suited for NLO research, because its structure comprises of electron donating and accepting groups. Due to the presence of electron donating groups in its structure, the dipole moment is significant, resulting in increased third-order nonlinearity. The optical nonlinearity of AG 50 dye can be increased owing to the structure flexibility.

Presently, laser pulses are effectively attenuated by organic materials, which protect human eyes and optical components from powerful light beams. These materials are intriguing due to their flexibility and transparency, as well as their ease of fabrication. An optical limiter greatly attenuates high-intensity laser pulses while remaining perfectly transparent at lower light levels. The output laser beam intensity saturates a certain intensity termed the limiting threshold, and the output laser beam intensity becomes clamped over the threshold. Even laser pointers with power ranges of 1–5 mW can injure the human eye if directly exposed for less than 0.25 s, mandating the usage of optical power limiters for low power CW lasers [18]. The delocalization of π-electrons has a strong relationship with the optical limiting behavior of organic compounds. An optical limiter can be made using a variety of nonlinear methods such as nonlinear absorption processes such as two photon absorption (TPA), free carrier absorption (FCA), saturable absorption (SA), reverse saturable absorption (RSA), and nonlinear refraction processes such as self-focusing, self-defocusing, photo refraction and optically induced scattering [19].

The present article is focused on the nonlinear absorption coefficient β (NLA) and optical limiting behavior of AG 50–PVA composite films using a CW diode laser radiation at 635 nm wavelength of 5 mW output power. NLA investigations reveal that the AG 50–PVA film have reverse saturable absorption (RSA) due to excited state absorption (ESA). The transparency and eco-friendly films of AG 50–PVA composites could be used in optoelectronic devices because of its tunable linear and nonlinear absorbance.

Experimental details

Materials

The polymer polyvinylalchol (PVA) with molecular weight of 125000 g mol^{-1}, the degree of hydrolysis of 86-89% (partially hydrolyzed grade) was purchased from Sigma Aldrich corporation, India and used as a host material for the present study. AG 50 dye ($C_{27}H_{25}N_2NaO_7S_2$) is a synthetic organic dye belongs to triarylmethane class with a molecular weight of 576.61 g mol^{-1} and the molecular structure of AG 50 dye is shown in Fig. 1.

Preparation of AG 50–PVA composite films

AG 50 dye–PVA composite films are prepared by solution casting technique. The PVA solution was prepared by dispersing 2 g of PVA powder in 100 ml of distilled water using a magnetic stirrer for 2 hours at 90°C/800 rpm without leaving any residues. In addition, different concentrations of AG 50 dye (0.01 mM, 0.02mM and 0.03 mM) were weighed and mixed with PVA solution and stirred for an hour to obtain a uniform solution. After that, the resulting mixture solution then casts onto the microslide glass plates and glass substrate was kept in a dark, clean environment for the formation of films. The good quality of films were obtained and further characterization studies were carried out.

Characterization methods

AG 50 dye–PVA composite thin films were examined by using a Perkin Elmer Lambda 35 spectrophotometer to measure the linear optical absorption. The crystal structure of AG 50 dye–PVA composite films were explored by PANalytical x-ray diffractometer using Cu-Kα radiation of wavelength 1.5406 Å in the 2θ range of 10–90° with stepping interval of 0.01°. FTIR spectra of AG 50–PVA composites in the range of 4000–400 cm-1 were collected on a Perkin-Elmer infrared spectrometer with an attenuated total reflectance (ATR). The morphology studies of AG 50–PVA composites were carried out using a scanning electron microscope (SEM) (CAREL ZEISS-EVO 18).

Mansoor Sheik Bahae et al., developed the simple Z-scan approach [20] which is extremely sensitive and

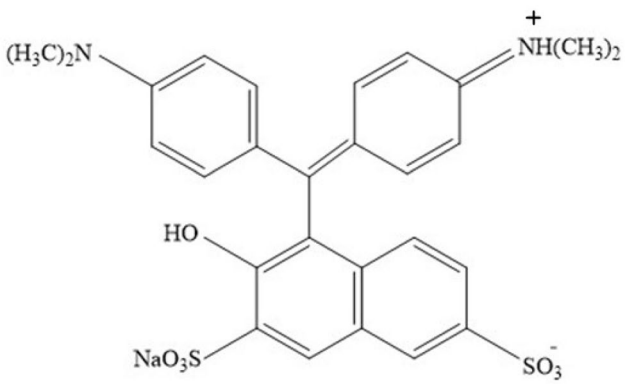

Molecular Formula: $C_{27}H_{25}N_2NaO_7S_2$

Fig. 1 Chemical structure and molecular formula of Acid green 50 dye

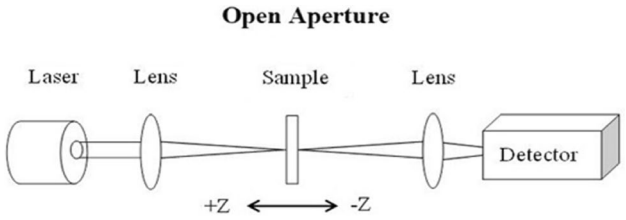

Fig. 2 Experimental set up for open aperture Z-scan measurements

straightforward was used for determining nonlinear optical properties of the material. This method can be used to calculate the sign and magnitude of the real and imaginary parts of third-order nonlinear optical susceptibility ($\chi^{(3)}$). The nonlinear optical absorption of AG 50–PVA composite films were examined using the open aperture (OA) Z-scan technique and illustrated in Fig. 2. The Z-scan method uses distortions in the spatial and temporal profile of the input laser beam as it passes through the sample to provide a descriptive and analytical measure of nonlinearities in the material medium. In the present work, we employed Z-scan measurements with continuous wave (CW) laser of Gaussian beam profile having 635 nm wavelength of 5 mW output power. The laser beam was tightly focused with the convex lens of 5 cm focal length, the beam size and the Rayleigh length (Z_R) are measured to be 16.75 µm and 1.38 mm, respectively. The input intensity of the laser beam at the focus was found to be of 1.135×10^3 Wcm^{-2}. An optical power meter (Field Master^{TM} GS, Coherent) was used to evaluate the beam transmittance through a sample without aperture. In the present case, the condition for the Rayleigh length $Z_R > L$ is achieved, hence the thin sample approximation is reasonably acceptable. The sample was placed at the focal plane of the lens in the same Z-scan experiment for optical power limiting measurements. A neutral density (ND) filter was used to vary the input intensity of the laser beam and the corresponding transmitted laser intensity through the sample was measured with an optical power meter.

Results and discussion

UV–visible studies

The linear absorption spectra of the aqueous solution of AG 50 dye (dotted lines), AG 50–PVA composite films at different dye concentrations of 0.01 mM, 0.02 mM and 0.03 mM respectively and pure PVA (inset) are shown in Fig. 3. From these figures we can infer that the absorption spectra of aqueous solution of AG 50 dye exhibit a broad absorption band with two peaks, which are located at wavelengths 372 nm and 634 nm and an absorbance of AG 50–PVA films are of 385 nm and 650 nm, respectively. There is a modest red

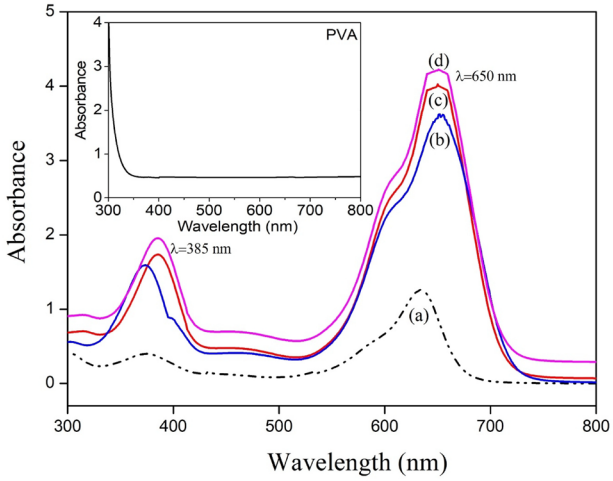

Fig. 3 UV–visible absorption spectra of (**a**) AG 50 dye in water of 0.01 mM and AG 50–PVA composite films at dye concentrations of (**b**) 0.01 mM, (**c**) 0.02 mM, (**d**) 0.03 mM, The inset: PVAfilm

shift of 14 nm in the absorption spectra when compared to both aqueous solution of AG 50 dye and AG 50–PVA composite films. The first absorbance spectra of both aqueous solution of AG 50 dye and AG 50–PVA films (i.e., 372 nm and 385 nm) are assigned to π-π* transitions which is due to the presence of π conjugated electrons in the aromatic rings [21, 22]. Similarly, the second absorbance spectra wavelength 634 nm and 650 nm are assigned to n-π*, π-π* transitions due to the excitation of C=O, C=C groups with electron donor and acceptor groups due to intermolecular hydrogen bonding between PVA and AG 50 dye molecule.

XRD studies

The XRD patterns of AG 50–PVA composite films with dye concentrations of 0.01 mM, 0.02 mM, and 0.03 mM, as well as pure PVA film (inset) and AG 50 dye molecules in powder form (inset) are shown in Fig. 4. The pure PVA (inset) diffraction pattern shows a diffraction band about $2\theta = 19.52°$ (corresponding to 110 plane) indicating that it is semicrystalline. This could be owing to significant intramolecular hydrogen bonding in individual PVA monomer units and intermolecular hydrogen bonding between monomer units. The AG 50 dye in powder form has multiple strong peaks at 2θ values of 31.72°,45.34°,56.29°66.26° and 75°, corresponding to the following lattice planes (200), (220), (222), (400) and (420) respectively indicating that it is crystalline in nature. The intensity of the main peak of the PVA in the AG 50–PVA composite films (see Fig. 5(a)–(c) reduced and became broader, indicating a decrease in crystallinity and exhibiting the occurrence of interaction between PVA chains and the organic dye filler molecules[23, 24]. This decrease in crystallinity, according to the literature, might be attributed

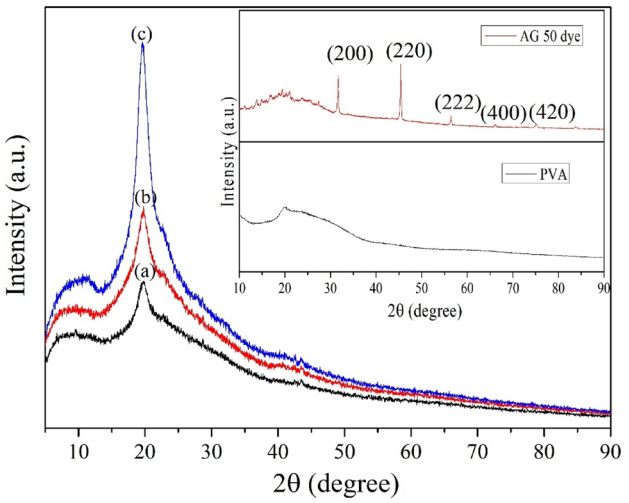

Fig. 4 XRD patterns of (**a**, **b** and **c**) AG 50–PVA composite films of dye concentrations 0.01 mM, 0.02 mM and 0.03 mM, respectively. The inset AG 50 dye in powder form and PVA film

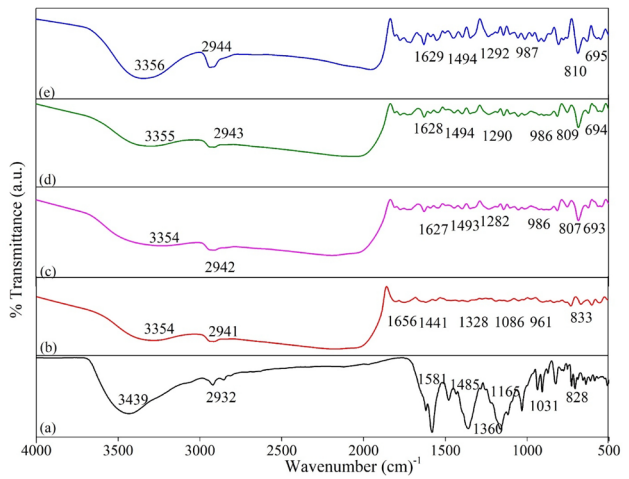

Fig. 5 FT–IR spectra of **a** AG 50 dye in powder form, **b** PVA film, (**c**, **d** and **e**) AG 50–PVA composite films with dye concentrations of 0.01 mM, 0.02 mM and 0.03 mM

to an increase in polymer electrolyte improves the flexibility of local chain metameric motion in the PVA host matrix. The Debye-Scherrer formula is used to compute the crystalline size of AG 50 dye in powder form:

$$D = \frac{0.9\lambda}{\beta\cos\theta}\text{nm} \quad (1)$$

where D is the crystalline size, λ is the X-ray wavelength radiation, θ is the Bragg diffraction angle and β is width at half maximum intensity (FWHM). The crystalline size of the AG 50 dye powder is computed to be 24.61 nm.

FT–IR analysis

The bonding structure and functional groups in AG 50–PVA composite films were characterized using FTIR spectroscopy. The FTIR spectra of AG 50 dye in powder form, pure PVA film, AG 50–PVA composite films with different dye concentrations of 0.01 mM, 0.02 mM and 0.03 mM respectively are shown in Fig. 5. The strong, broad absorption band at 3354 cm^{-1} caused by O-H vibrational stretching in pure PVA is slightly moved to 3354 cm^{-1}, 3355 cm^{-1} and 3356 cm^{-1} respectively for with different dye concentrations of 0.01 mM, 0.02 mM and 0.03 mM signifying that AG 50 dye molecules may interact with the hydroxyl group of the PVA. The sharp peaks at 2941 cm^{-1}, 2942 cm^{-1}, 2943 cm^{-1} and 2944 cm^{-1} in the pure PVA as well as in AG 50–PVA composite films of 0.01 mM, 0.02 mM and 0.03 mM are ascribed to C-H asymmetric stretching. The shift of the transmittance bands observed in pure PVA at 1656 cm^{-1} corresponds to C=C vibration stretching whereas absorption bands present at 1627 cm^{-1}, 1628 cm^{-1} and 1629 cm^{-1} for AG 50–PVA composite films with different dye concentrations of 0.01 mM, 0.02 mM and 0.03 mM respectively corresponds to N-H bend amine group due to decrease in intensity after the accumulation of AG 50 dye, imply intramolecular or intermolecular hydrogen bonding and complex formation [25, 26]. The absorption band 1441 cm^{-1} at pure PVA which seems to shift at 1493 cm^{-1} and 1494 cm^{-1} in the AG 50–PVA composite films is due to N-O asymmetric stretching in the AG 50 dye molecule. The observed peak at 1328 cm^{-1} of pure PVA and absorbance band of AG 50–PVA composite films of 0.01 mM, 0.02 mM and 0.03 mM, respectively, at 1282 cm^{-1},1290 cm^{-1} and 1292 cm^{-1} of assigned to C-N stretching amines. The considerable peaks in the pure PVA and AG 50–PVA composite films at 833 cm^{-1} and 807 cm^{-1}, 809 cm^{-1} and 810 cm^{-1}, respectively, due to C-H bending. In the AG 50–PVA composite films, the peaks at 693, 694 and 695 are attributed to C=C bending of alkenes.

SEM analysis

The surface morphology of AG 50–PVA composite films with different dye concentrations of 0.01 mM, 0.02 mM and 0.03 mM were studied using a scanning electron microscope (SEM). The morphological SEM images are shown in Fig. 6. The 0.01 mM AG 50–PVA composite films possesses a smooth surface and uniform distribution subsequently including the AG 50 dye with PVA. However, the composite AG 50–PVA with 0.02 mM dye concentration has shown a smooth surface with even spreading of globular bunches and hovels exist, in which the bubbles are occurred during the film preparation. The interaction between the PVA and AG 50 dye restricts the accumulation of dye molecules in the PVA matrix at a lower doping level [27].

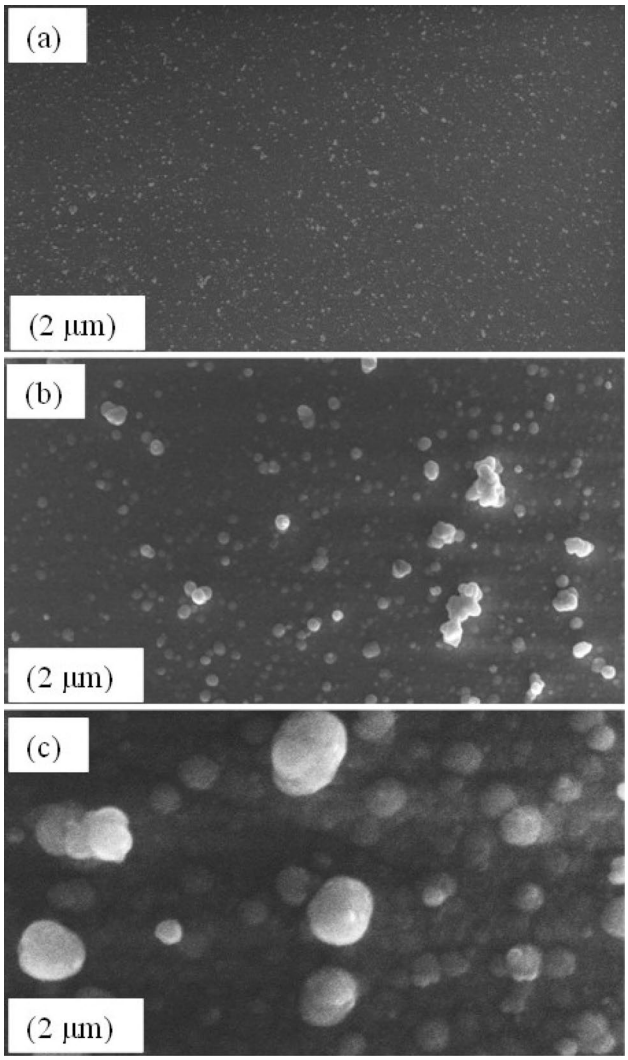

Fig. 6 SEM micrographs of AG 50–PVA composite films **a** 0.01 mM, **b** 0.02 mM and **c** 0.03 mM

Nonlinear absorption

An open aperture Z–scan experiment with input intensity $I_0 = 1.135 \times 10^3$ Wcm^{-2} was used to examine the intensity dependence of the nonlinear absorption method of AG 50–PVA composite films with different dye concentrations of 0.01 mM, 0.02 mM, and 0.03 mM, as well as the aqueous solution of AG 50 dye (0.01 mM). Fig. 7 shows the open aperture Z–scan traces of AG 50–PVA composite films and aqueous solution of AG 50 dye. The study of AG 50–PVA composite films and aqueous solution of AG 50 dye (0.01 mM) are positioned on the translation stage and made to turn from one end of the far field to the other end through focus. The laser intensity is low when the samples are in the far field, hence the normalized transmittance value will be one or unity. As the sample approaches the focus, the transmittance value drops, forming a dip or valley at the focus (Z=0). This decrease in the transmittance value indicates the occurrence of reverse saturable absorption (RSA) behavior or positive nonlinear absorption. Furthermore, as the incident laser intensity at the focus increases, the dip or valley transmission get decreased. Nonlinear mechanisms such as two photon absorption (TPA), excited state absorption (ESA), free carrier absorption, nonlinear scattering, or a combination of these processes can induce RSA [28, 29]. Fig. 8 shows the five level energy diagram of AG 50 dye molecules. TPA is the absorption of two photons with the same or different energy values from the ground level to the excited level state in an instant (S_0-S_1). This energy conversion procedure can be achieved is equal to the sum of two photon absorption. ESA is a process in which molecules make a transition from the first level excited state to a higher level excited state (S_1-S_2) or vice versa (T_1-T_2). To do so, the population of first level excited states (S_1 and/or T_1) must be massive enough to increase the likelihood of absorption of photon from the state. As the electrons from the first level singlet excited state S_1 are transferred to the first level triplet excited state T_1 via intersystem crossing (ISC), transitions to higher level excited state T_2 are possible, hypothetically enhances the ESA or RSA [30]. Hence, in the present case the excited thermal effects caused by CW laser excitation rise ESA, inferring that ESA-assisted RSA is the major cause which was observed in the nonlinearity of AG 50 dye molecules.

The normalized transmittance from open aperture Z-scan method is represented by

$$T(z, s = 1) = \sum\nolimits_{m=0}^{\infty} \frac{\left[-q_0(z)\right]^m}{[m+1]^{\frac{3}{2}}}, for\ \left|q_0(0)\right| < 1 \tag{2}$$

where

$$q_0(z) = \frac{\beta_{eff} I_0 L_{eff}}{1 + \frac{z^2}{z_0^2}} \tag{3}$$

where β_{eff} is the nonlinear absorption coefficient obtained from open aperture Z-scan data is given by $\beta_{\text{eff}} = \frac{2\sqrt{2}\Delta T}{I_0 L_{\text{eff}}}$, Here, L_{eff} is the effective thickness of the sample, which is defined as, $L_{\text{eff}} = \frac{(1-e^{-\alpha L})}{\alpha}$. Here, I_o is the focal point beam intensity of the laser, α is the linear coefficient of absorption, Z_0 is the diffraction length and L is the sample thickness. The imaginary parts of the third-order NLO susceptibility $\chi^{(3)}$ is given by,

$$\mathrm{Im}\left[\chi^{(3)}\right](\mathrm{esu}) = \frac{\varepsilon_0 c^2 n_0^2 \lambda}{4\pi^2} \beta \times 10^{-2} \left(\frac{\mathrm{cm}}{\mathrm{W}}\right) \tag{4}$$

where ε_0 = free space permittivity, c = velocity of light, n_0 = linear refractive index, λ = wavelength of light. The measured NLO parameters such as nonlinear absorption

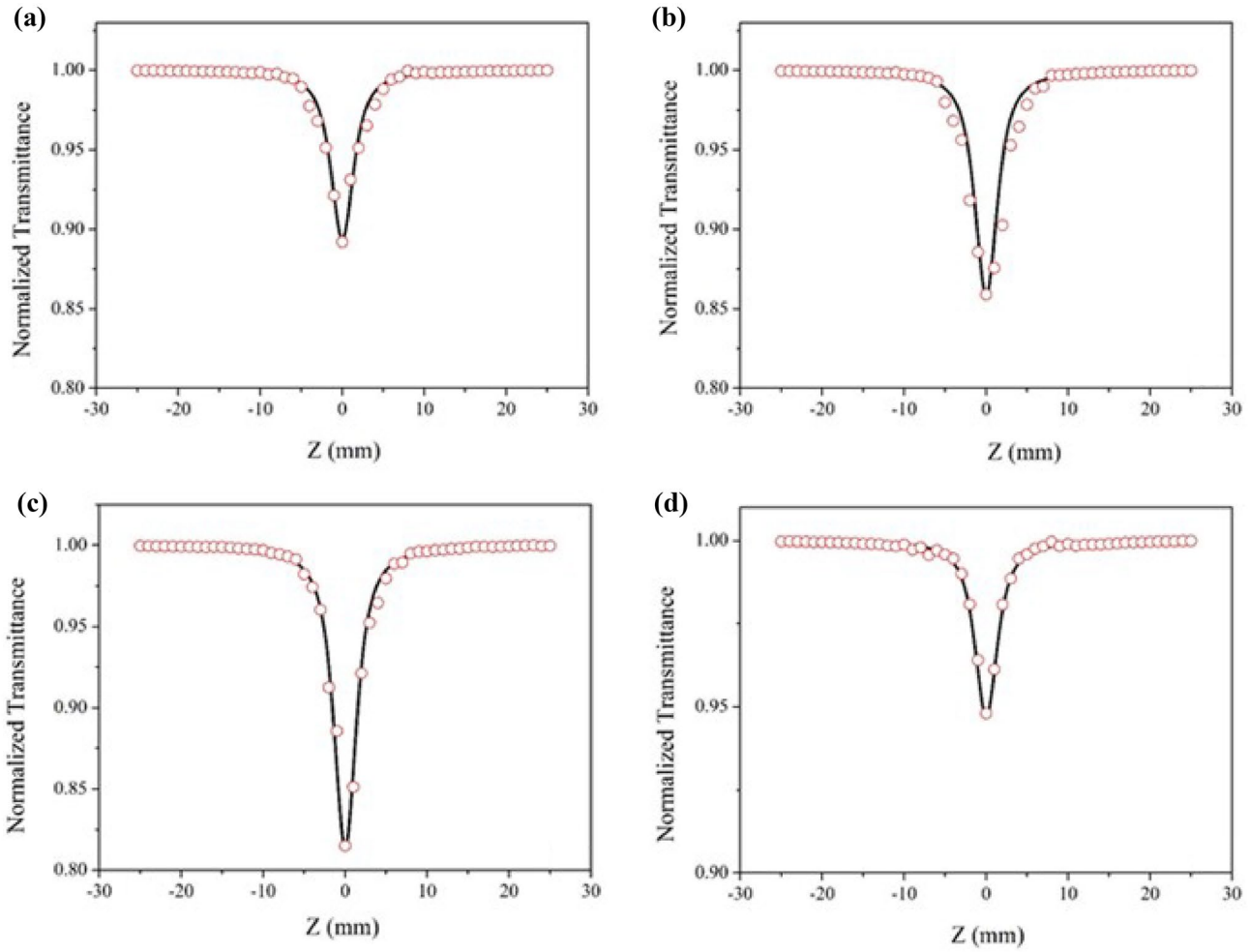

Fig. 7 Open aperture Z-scan curve for AG 50–PVA composite films with dye concentrations of **a** 0.01 mM, **b** 0.02 mM and **c** 0.03 mM and **d** AG 50 dye in water (0.01 mM)

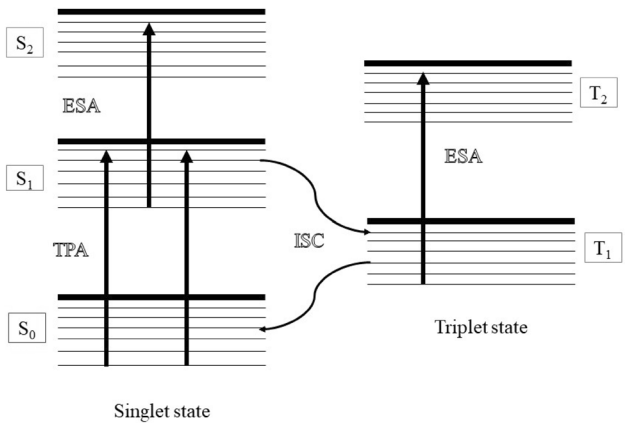

Fig. 8 Five level model energy diagram for AG 50 dye molecule

coefficient β and imaginary parts of the third-order NLO susceptibility $\chi^{(3)}$ for AG 50–PVA composite films and aqueous solution of AG 50 dye are given in Table 1.

Table 1 Measured nonlinear absorption parameters of AG 50–PVA composite films and AG 50 dye in water (Incident intensity $I_0 = 1.135 \times 10^3$ W/cm^2)

Sample	Dye concentration (mM)	β (cm/W)	Im$\chi^{(3)}$ I$\times 10^{-5}$ (e.s.u)
AG 50–PVA	0.01	0.148	3.37
AG 50–PVA	0.02	0.201	4.56
AG 50–PVA	0.03	0.256	5.82
AG 50–water solution	0.01	1.517×10^{-3}	0.034

Optical limiting

Optical limiting occurs when the input beam intensity exceeds a certain threshold, so called the limiting threshold. The materials endure this behavior are called as optical limiters. Many organic, inorganic, thin films, nano particle encapsulated materials and semiconducting materials has

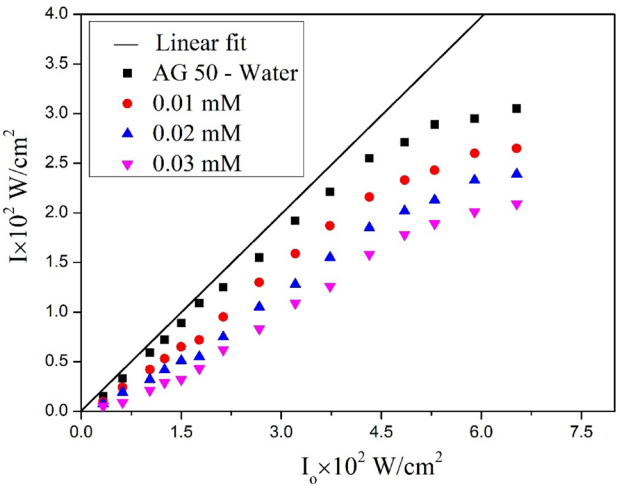

Fig. 9 Optical limiting characteristics of AG 50–PVA composite films

Table 2 Optical limiting parameters of AG 50–PVA composite films and AG 50 dye in water

Sample	Dye concentration (mM)	Optical limiting threshold ($I \times 10^2$ W/cm^2)
AG 50–water solution	0.01	2.14
AG 50–PVA	0.01	1.78
AG 50–PVA	0.02	1.70
AG 50–PVA	0.03	1.49

been examined to accomplish optical limiting. The protection of eyes and sensors has greatly improved as a result of the use of high-power lasers. The open aperture Z–scan technique was used to characterize the optical limiting effect of aqueous solution of AG 50 dye (0.01 mM) and AG 50–PVA composite films with different dye concentrations of 0.01 mM, 0.02 mM and 0.03 mM are presented in Fig. 9. A neutral density filter (NDF) is exploited to differ the laser beam input intensity and consequently transmitted intensity was determined by using a digital power meter. The sample under study are kept precisely at the focal plane of lens and the corresponding transmitted power of different input powers are determined. It is clear that the output beam intensity differs linearly with respect to low incident input beam intensity and the linear transmittance obeyed Beer–Lambert's law, $I = I_0 e^{-\alpha L}$, where I_0 is the input beam intensity, I is output beam intensity, α is the linear absorption coefficient and L is the thickness of the sample. The measured values of optical limiting threshold for aqueous solution of AG 50 dye (0.01 mM) and AG 50–PVA composite films of different dye concentrations of 0.01 mM, 0.02 mM and 0.03 mM are tabulated in Table 2. It is clear from Table 2 the lower limiting threshold of 1.49×10^2 Wcm^{-2} was observed with 0.03 mM concentration. The limiting threshold values are also inversely proportional to the dye sample concentration. As there is a rise in concentration, particles per unit volume contributed in the interface and they are thermally agitated to excited state and hence improved limiting threshold is observed. Several nonlinear optical mechanisms are included to achieve optical limiting process such as self-focusing, self-defocusing, excited state absorption (ESA), two photon absorption (TPA), free carrier absorption (FCA) in nonlinear media [31, 32]. Our present sample is an energy absorbing type of optical limiter and the major nonlinear mechanism employed is ESA-assisted RSA process.

Conclusion

AG 50–PVA composite films of different dye concentrations were prepared by solution casting technique, their optical absorption, structural and morphological details were studied. The nonlinear absorption (NLA) and optical limiting (OL) behavior of AG 50–PVA composite films of different dye concentrations and aqueous solution of AG 50 dye (0.01 mM) were also studied. The optical absorption spectra reveals strong linear absorption at 650 nm wavelength due to the presence of π–conjugated electrons in the AG 50 dye molecules. The XRD results illustrates that AG 50–PVA composite films exhibits semicrystalline nature and FT–IR study demonstrates the bonding nature and functional groups present in the AG 50 dye molecules and PVA. The morphological studies confirms the even distribution of AG 50 dye molecules within the PVA host matrix. The open aperture Z-scan has been performed with a continuous wave diode laser (CW) at 635 nm wavelength and 5 mW output power exposed that reverse saturable absorption in both AG 50–PVA composite films and as well as aqueous solution of AG 50 dye. AG 50–PVA composite films exhibits a high optical limiting efficiency based on strong reverse saturable absorption at 635 nm wavelength, for the protection of human eye and sensor devices.

References

1. M.A. Kramer, W.R. Tompkin, R.W. Boyd, Nonlinear-optical interactions in fluorescein-doped boric acid glass. Phys. Rev. A **34**, 2026–2031 (1986)
2. K. Jamshidi-Ghaleh, S. Salmani, M.H. Majlesara, Nonlinear responses and optical limiting behavior of fast green FCF dye under a low power CW He–Ne laser irradiation. Opt. Commun. **271**, 551–554 (2007). https://doi.org/10.1016/j.optcom.2006.10.037
3. J.L. Bredas, C. Adant, P. Tackx, A. Persoons, Third-order nonlinear optical response in organic materials: theoretical and experimental aspects. Chem. Rev. **94**, 243–278 (1994). https://doi.org/10.1021/cr00025a008

4. T. Geethakrishnan, P. Sakthivel, P.K. Palanisamy, Triphenylmethane dye-doped gelatin films for low-power optical phase-conjugation. Opt. Commun. **335**, 218–223 (2015). https://doi.org/10.1016/j.optcom.2014.09.033
5. T. Geethakrishnan, P.K. Palanisamy, Z-scan determination of the third-order optical nonlinearity of a triphenylmethane dye using 633 nm He–Ne laser. Opt. Commun. **270**, 424–428 (2007). https://doi.org/10.1016/j.optcom.2006.09.035
6. T. Wang, X. Wang, J. Zhang, C. Wang, J. Shao, Z. Jiang, Y. Zhang, Synthesis, structure and third-order optical nonlinearities of hyperbranched metal phthalocyanines containing imide units. Dyes Pigments **154**, 75–81 (2018). https://doi.org/10.1016/j.dyepig.2018.02.031
7. M. Ghanipour, D. Dorranian, Effect of Ag-Nanoparticles Doped in Polyvinyl Alcohol on the Structural and Optical Properties of PVA Films. J. Nanomater **2013**, 1–10 (2013). https://doi.org/10.1155/2013/897043
8. S. Mahendia, A.K. Tomar, R.P. Chahal, P. Goyal, S. Kumar, Optical and structural properties of poly(vinyl alcohol) films embedded with citrate-stabilized gold nanoparticles. J. Phys. D Appl. Phys. **44**, 1–8 (2011). https://iopscience.iop.org/0022-3727/44/20/205105
9. K.M. Manikandan, A. Yelilarasi, P. Senthamaraikannan, S. Saravanakumar, A. Khan Abdullah, A study on optical limiting properties of Eosin-Y and Eriochrome Black-T dye-doped poly (vinyl alcohol) composite film. Int. J. Polym. Anal. Charact. **326**, 1–8 (2019). https://doi.org/10.1080/1023666X.2019.1596366
10. H. Eskalen, H. Yaykas, M. Kavgac, A. Kayıs, Investigating the PVA/TiO2/CDs polymer nanocomposites: effect of carbon dots for photocatalytic degradation of Rhodamine B. J Mater Sci: Mater Electron. **33**, 4643–4658 (2022). https://doi.org/10.1007/s10854-021-07653-0
11. V. Hebbar, R.F. Bhajantri, J. Naik, S.G. Rathod, Thiazole yellow G dyed PVA films for optoelectronics: microstructrural, thermal and photophysical studies Mater. Mater. Res. Express **3**, 1–16 (2016). http://iopscience.iop.org/2053-1591/3/7/075301
12. H. Esfahani, M. Ghanipour, D. Dorranian, Effect of dye concentration on the optical properties of red-BS dye-doped PVA film. J. Theor. Appl. Phys. **8**, 117–121 (2014). https://doi.org/10.1007/s40094-014-0139-3
13. K.S. Hemalatha, K. Rukmani, N. Suriyamurthy, B.M. Nagabhushana, Synthesis, characterization and optical properties of hybrid PVA–ZnO nanocomposite: a composition dependent study. Mater. Res. Bul. **51**, 438–446 (2014). https://doi.org/10.1016/j.materresbull.2013.12.055
14. M.H. Anandalli, R.F. Bhajantri, S.R. Maidur, P.S. Patil, Fluorescence and third-order nonlinear optical properties of thermally stable CBPEA dye-doped PMMA/ZnO nanocomposites. J. Mater. Sci.: Mater. Electron. **31**, 10531–10547 (2020). https://doi.org/10.1007/s10854-020-03601-6
15. V. Ovdenko, D. Vyshnevsky, N. Davidenko, I. Davidenko, V. Pavlov, Effect of molecular weight of PEG polymer matrix on the diffraction efficiency of Methyl Orange holographic media. Opt. Mater. **2020**, 1–8 (2020). https://doi.org/10.1016/j.optmat.2020.110549
16. S. Mondal, A. Verma, S. Saha, Eur. Conformationally restricted triarylmethanes: synthesis, photophysical studies, and applications. J. Org. Chem. **2019**, 864–894 (2019)
17. B. Pathrose, V.P.N. Nampoori, P. Radhakrishnan, A. Mujeeb, Investigations on the third order nonlinear optical properties of Basic Fuchsin dye using z scan technique. Optik (Stuttg.) **2016**, 1–21 (2016). https://doi.org/10.1016/j.ijleo.2016.05.136
18. D. Narayana Rao, C.S. Yelleswarapu, S.R. Kothapalli, D.V.G.L.N. Rao, B.R. Kimball, Self-diffraction in bacteriorhodopsin films for low power optical limiting. Opt. Express **11**, 2848–2853 (2003). https://doi.org/10.1364/OE.11.002848
19. S. Zongo, K. Sanusi, J. Britton, P. Mthunzi, T. Nyokong, M. Maaza, B. Sahraoui, Nonlinear optical properties of natural laccaic acid dye studied using Z-scan technique. Opt. Mater. **46**, 270–275 (2015). https://doi.org/10.1016/j.optmat.2015.04.031
20. M. Sheik-Bahae, A.A. Said, T. Wei, D.J. Hagan, E.M. Van Stryland, Sensitive measurement of optical nonlinearities using a single beam. IEEE. J. Quant. Elect. **26**, 760–769 (1990). https://doi.org/10.1109/3.53394
21. L. Guru Prasad, Azo Dye doped polymer films for nonlinear optical applications Chinese. Chin. J. Polym. Sci. **32**, 650–657 (2014). https://doi.org/10.1007/s10118-014-1441-x
22. A. Migalska Zalas, K.E.L. Korchi, T. Chtouki, Enhanced nonlinear optical properties due to electronic delocalization in conjugated benzodifuran derivatives. Opt. Quantum Electron. **50**, 1–10 (2018). https://doi.org/10.1007/s11082-018-1659-x
23. P. Settu, G. Gobi, P. Baskaran, N. Renuka, Effect of Leishman stain on synthesis, characteristics, and morphology of $Zn_{0.15}Cd_{0.8}S_{0.8}$ thin film. J. Electron. Mater. **49**, 4160–4167 (2020). https://doi.org/10.1007/s11664-020-08130-w
24. R. Das, R. Kumar, Preparation of nanocrystalline PbS thin films and effect of Sn doping and annealing on their structural and optical properties. Mater. Res. Bull. **47**, 239–246 (2012). https://doi.org/10.1016/j.materresbull.2011.11.025
25. V. Krishnakumar, R. Ranjith, J. Jayaprakash, S. Boobas, J. Venkatesan, Enhancement of photocatalytic degradation of methylene blue under visible light using transparent Mg-doped CdS–PVA nanocomposite films. J. Mater. Sci. Mater. Electron. **28**, 13990–13999 (2017). https://doi.org/10.1007/s10854-017-7249-z
26. R. Bisen, J. Tripathi, A. Sharma, A. Khare, Y. Kumar, S. Tripathi, Optical behaviour of coumarin dye in PVA and PMMA film matrices. Vacuum **2018**, 1–20 (2018). https://doi.org/10.1016/j.vacuum.2018.03.004
27. N. George, R. Subha, N.L. Mary, A. George, V. Anoop, Functionalized electrospun nanofibers integrated with Ag/Au nanoparticles as a platform for enhanced nonlinearity. Opt. Quantum Electron **54**, 1–15 (2022). https://doi.org/10.1007/s11082-022-03538-6
28. T. Geethakrishnan, P.K. Palanisamy, Generation of phase-conjugate wave in acid blue 7 dye-doped gelatin film. Curr. Sci. **89**, 1894–1898 (2005)
29. R. Madhana Sundari, P.K. Palanisamy, Self-diffraction and Z-scan studies in organic dye doped thin films. Appl. Surf. Sci. **252**, 2281–2287 (2006). https://doi.org/10.1016/j.apsusc.2005.04.017
30. S. Jeyaram, S. Hemalatha, T. Geethakrishnan, Nonlinear refraction, absorption and optical limiting properties of disperse blue 14 dye. Chem. Phys. Lett. **2019**, 1–15 (2019). https://doi.org/10.1016/j.cplett.2019.137037
31. R.K. Choubey, S. Medhekar, R. Kumar, S. Mukherjee, S. Kumar, Study of nonlinear optical properties of organic dye by Z-scan technique using He–Ne laser. J. Mater. Sci. Mater. Electron. **25**, 1410–1415 (2014). https://doi.org/10.1007/s10854-014-1743-3
32. O. Muller, C. Hedge, M. Guerchoux, L. Merlat, Synthesis, characterization and nonlinear optical properties of polylactide and PMMA based azophloxine nanocomposites for optical limiting applications. J. Mater. Sci. Eng. B **276**, 1–11 (2022). https://doi.org/10.1016/j.mseb.2021.115524